Bio-Inspired Stiffness Control for Cable-Driven Parallel Robots

Dragos Mihai PANAGORET[1], Andreea Anamaria PANAGORET[1]*, Olivia-Roxana ALECSOIU[2], Maria Felicia CHIRCULESCU[2], Adina-Milena TATAR[2]

[1] Valahia University of Târgovişte, Târgovişte, 130004, Romania
panagoret_dragos@yahoo.com, andreea_panagoret@yahoo.com (**Corresponding author*)

[2] Constantin Brâncusi University of Târgu Jiu, Târgu Jiu, 210185, Romania
oliviaalecsoiu@gmail.com, chirculescu_felicia@yahoo.com, adynatatar@gmail.com

Abstract: This paper presents an advanced bio-inspired control framework for cable-driven parallel robots (CDPRs), based on the principle of agonist–antagonist biomechanical coordination specific to the human muscular system. The proposed architecture introduces a variable stiffness regulation strategy, in which cable tensions are dynamically adjusted so as to reproduce the contraction and relaxation behaviors specific to myofibrillar structures. The control model employs a deterministic mechanical adaptation law, formulated in terms of positional deviation and force variation, through which the equivalent stiffness of the system can adjust itself in real time, without depending on empirical models or machine learning algorithms. The experimental validation was performed on a CDPR platform with eight redundant cables, configured for full-scope simulations and laboratory tests in the hardware-in-the-loop (HIL) mode. The experiments included controlled interactions with a biomechanical phantom designed to reproduce the elastic properties of biological tissues, allowing for the precise assessment of the stability, precision, and dynamic behavior of the system. The obtained results include a 2.6 mm RMS error in trajectory tracking and a maximum contact force below 25 N, indicating a stable, safe, and adaptive operating regime. The integration of biomechanical principles into the control architecture of cable-driven parallel robots points the way towards a new generation of intelligent actuator systems, capable of combining mechanical precision with structural adaptability, ensuring remarkable application perspectives in the fields of rehabilitation robotics, delicate manipulation, and collaborative robotics.

Keywords: Cable-actuated parallel robots, Bio-inspired control, Variable stiffness control, Mechanical safety, Adaptive control, Full-scope simulation, Conformal robotics.

1. Introduction

Robotic systems for motor rehabilitation have become an important research direction in biomedical engineering and rehabilitation mechatronics due to their ability to provide repetitive, quantifiable, and patient-specific therapeutic assistance (Shah et al., 2023; Li et al., 2023). These systems support physiotherapists by enabling controlled neuromuscular training based on measurable biomechanical parameters (Marinescu et al., 2025). Among the existing rehabilitation architectures, Cable-Driven Parallel Robots (CDPRs) have attracted increasing interest because of their low moving inertia, large workspace, high force-to-weight ratio, and intrinsic compatibility with human limb movements.

Unlike the conventional rigid-link robotic architectures, cable-driven parallel robots (CDPRs) transmit forces and moments through tension cables connecting a mobile platform to a fixed supporting structure (Wang et al., 2025; Hong et al., 2018). This mechanical configuration provides several important advantages, including a reduced moving inertia, a lower structural mass, a high force-to-weight ratio, and the ability to generate smooth multidirectional motions with an improved dynamic responsiveness. Owing to these characteristics, CDPR systems have been successfully implemented in applications ranging from industrial manipulation and aerospace engineering to medical robotics and rehabilitation systems. Representative platforms such as CAREX, C-ALEX, TruST, and A-TPAD have demonstrated the ability of CDPR architectures to support limb rehabilitation, gravitational unloading, and neuromuscular coordination training through controlled and compliant interaction mechanisms (Runciman et al., 2020; Tada & Sumiyama, 2024). These developments confirm the growing relevance of CDPR systems in rehabilitation-oriented robotics, particularly in applications requiring safe physical interaction and adaptive force regulation.

The performance of the CDPR systems critically depends on the adopted control strategy. The simultaneous regulation of platform motion and cable tension remains a challenging problem due to cable unilateral actuation, kinematic redundancy, nonlinear elastic behavior, and coupling between force and position dynamics. Consequently, extensive research has focused on improving the CDPR performance through advanced kinematic

https://doi.org/10.24846/v35i2y202609

optimization, workspace enhancement, vibration suppression, dynamic parameter identification, and adaptive force control approaches (Sun et al., 2020; Harandi et al., 2022). The existing studies indicate that the positioning accuracy and dynamic stability are strongly influenced by the fidelity of the underlying dynamic models and by the controller capability to compensate for the disturbances generated by friction, inertia variations, cable elasticity, and external loading conditions (Wang et al., 2025; Shah et al., 2023).

The existing CDPR control strategies can generally be categorized into classical PID-based control, impedance/admittance control, adaptive control, and model predictive control (MPC) frameworks. Conventional PID and computed-torque control approaches provide a satisfactory performance under static or slightly nonlinear operating conditions but exhibit a limited robustness in the presence of variable interaction forces and cable elasticity (Ren et al., 2022).

Impedance and admittance control methods improve interaction safety and compliance; however, they rely heavily on accurate environment and dynamic parameter estimation (Yang et al., 2025). More advanced adaptive and MPC-based controllers achieve superior disturbance rejection and predictive regulation capabilities but they often require computationally intensive optimization procedures and extensive online parameter identification, which may limit their real-time implementation in rehabilitation-oriented robotic systems.

Recent developments in rehabilitation robotics increasingly emphasize compliant interaction and adaptive impedance regulation as essential requirements for a safe human–robot interaction. In cable-driven rehabilitation systems, achieving a stable interaction behavior remains particularly challenging because cable elasticity, force redistribution, and biomechanical coupling generate strongly nonlinear dynamic responses. Consequently, the current research trends focus on adaptive stiffness regulation frameworks capable of simultaneously improving interaction safety, dynamic stability, and robustness to external disturbances while reducing the dependence on highly parameterized dynamic models.

In the field of force regulation, two principal approaches are commonly employed: direct force control based on real-time cable tension feedback and indirect control achieved through actuator position or velocity regulation. Classical controllers remain effective in quasi-static operating regimes, such as isometric rehabilitation exercises, but their performance deteriorates under dynamic interaction conditions characterized by variable loads and nonlinear biomechanical responses (Niresh et al., 2019). To compensate for these limitations, many studies have incorporated empirical friction compensation models or experimentally identified dynamic parameters. Although such methods improve local performance, they often reduce reproducibility and robustness when operating under varying biomechanical conditions or unpredictable external disturbances (Villalobos et al., 2023; Saidi et al., 2019).

Dynamic modeling approaches based on spring-damper representations of cable elasticity have significantly improved the understanding of CDPR behavior in dynamic operating conditions and enabled the development of higher-order controllers with enhanced stability characteristics (Najafi & Spencer, 2019; Alagoz et al., 2020). Zhang et al. (2019) demonstrated that the accurate modeling of the transfer relationship between motor torque and cable tension enables a precise force regulation; however, such approaches require an extensive identification of dynamic and friction-related parameters. Consequently, recent research trends increasingly focus on control architectures capable of reducing the dependence on highly detailed system models while preserving the adaptive mechanical behavior and stable interaction dynamics.

Despite these advances, an important limitation remains insufficiently addressed in the current literature: most existing CDPR control strategies still depend on highly parameterized dynamic models or experimentally identified compensation terms that are difficult to generalize across different biomechanical interaction scenarios (Gu & Ren, 2023; Wang et al., 2025). As a consequence, controller robustness may deteriorate in the presence of variable external loads, nonlinear tissue interaction, or unmodeled dynamic disturbances.

Biologically inspired control concepts provide a promising alternative for addressing these

limitations because biological musculoskeletal systems achieve stable and adaptive mechanical responses through the continuous modulation of stiffness, damping, and force distribution rather than through an exact dynamic model compensation. Translating these mechanisms to CDPR architectures may improve the adaptive interaction behavior while preserving the computational simplicity and real-time implementation capability.

To address these limitations, the present study proposes a bio-inspired adaptive stiffness control framework for cable-driven parallel robots, aimed at reducing the dependence on highly detailed dynamic models while preserving a stable force regulation and safe mechanical interaction. The proposed approach is inspired by the biomechanical coordination mechanisms of agonist-antagonist muscle pairs, in which force generation and passive stabilization coexist through dynamically regulated stiffness responses. Translating this principle to CDPR systems enables a coordinated cable actuation, where the selected cables generate an active motion while the complementary cable groups provide an adaptive stabilization through tension redistribution.

The proposed methodology develops and experimentally validates a bio-inspired variable stiffness control strategy for cable-actuated parallel robots, capable of adapting the equivalent mechanical stiffness of the system in real time according to load variations and platform dynamic states. The originality of this approach lies in the formulation of a deterministic adaptive stiffness law derived from biomechanical interaction principles, enabling the simultaneous regulation of cable tension distribution and equivalent stiffness as functions of positional deviation and measured interaction forces.

In addition, a Dynamic Safety Envelope framework is introduced in order to define the admissible operating limits for cable tensions, equivalent stiffness, and interaction forces during robot operation. The proposed framework continuously constrains the system dynamics within predefined biomechanical safety boundaries, reducing the risk of unstable operating conditions or excessive mechanical loading. The experimental validation was conducted using an eight-cable CDPR platform integrated with a full-scope simulation environment combining dynamic modeling, sensor feedback, and a real-time control architecture. The methodology was evaluated using a biomechanical phantom reproducing viscoelastic tissue behavior, allowing a safe and reproducible assessment of stiffness adaptation, force regulation, and system stability without human-subject involvement.

The main contributions of this work are summarized as follows:

a. A bio-inspired adaptive stiffness control law for cable-driven parallel robots is proposed based on agonist-antagonist cable coordination and real-time stiffness modulation;

b. A Dynamic Safety Envelope framework is introduced to maintain cable tensions, equivalent stiffness, and interaction forces within predefined biomechanical safety limits;

c. A hierarchical control architecture integrating local tension regulation and global stiffness adaptation is implemented in real time using an EtherCAT-based control system;

d. The proposed method is experimentally validated on an eight-cable CDPR platform using a biomechanical phantom reproducing viscoelastic tissue properties;

e. Comparative experiments against conventional PID control demonstrate reductions in the value of RMS force error, overshoot, and settling time together with an improved energy efficiency and force stability;

f. Unlike the conventional model-dependent control approaches, the proposed framework reduces the reliance on an extensive parameter identification while preserving an adaptive and stable robot-environment interaction.

The working hypothesis of this study is that adaptive stiffness regulation based on biomechanical interaction principles can achieve a positioning accuracy and force stability comparable with those obtained by the established control methods while reducing the dependence on highly detailed dynamic models and empirical friction compensation strategies.

The proposed methodology was validated through numerical simulations and controlled experimental testing using a biomechanical phantom under multiple loading scenarios. The

obtained results demonstrate a stable adaptive behavior, a reduced positioning error, and safe force regulation under dynamic operating conditions. Although the current validation was performed under controlled laboratory conditions and moderate dynamic regimes, the proposed framework represents a reproducible basis for future extensions toward more complex rehabilitation-oriented robotic interactions.

The remainder of the paper is organized as follows: Section 2 presents the theoretical foundations, dynamic models, and the formulation of the bio-inspired control law. Section 3 describes the experimental system architecture, test platform, and implementation procedure. Further on, Section 4 sets forth the simulation and experimental results together with the corresponding performance analysis, while Section 5 discusses the obtained results and their implications relative to the existing CDPR control approaches. Finally, Section 6 presents the conclusions of this paper and outlines future research directions.

2. Theoretical Framework

The theoretical analysis of the proposed control framework is based on the kinematic and dynamic modeling of the cable-actuated parallel robot, aiming at the precise description of the relationship between the movement of the mobile platform, the distribution of tensions in the cables, and the equivalent mechanical stiffness of the assembly. The considered configuration includes a mobile platform connected to a fixed base by a system of tension cables, each cable being driven independently by an electric motor with controlled torque (Zhang et al., 2019; Hong et al., 2018). The resulting structure ensures an extended mobility, a reduced mass of the moving elements, and a low inertia, allowing the precise regulation of the movement through the coordinated distribution of tensions.

In the case of a cable-actuated parallel robot, the kinematic relationship between the lengths of the cables and the position of the platform is nonlinear, and the determination of the corresponding tensions to maintain balance requires a rigorous mathematical description (Sun et al., 2020; Li et al., 2023). The cable velocities and the platform velocities are correlated through the Jacobian matrix J, which expresses the correspondence between the movement of the joints and the movement of the platform:

$$\dot{\mathrm{I}} = \mathrm{J}\dot{\mathrm{p}} \tag{1}$$

where $\dot{\mathrm{I}}$ denotes the vector of the winding speeds of the cables, and $\dot{\mathrm{p}}$ represents the vector of the linear and angular speeds of the platform. Under the conditions of static equilibrium, the forces transmitted to the platform can be expressed by the relation:

$$\mathrm{F}_p = \mathrm{J}^T\mathrm{T} \tag{2}$$

where $\mathrm{T} = [T_1, T_2, ..., T_n]^T$ is the stress vector, and F_p represents the resultant vector of the forces applied to the platform.

Maintaining mechanical stability requires the existence of a set of strictly positive tensions capable of ensuring equilibrium and preventing cable relaxation. Consequently, the control of the equivalent stiffness becomes a fundamental parameter for adaptive compliance and mechanical safety in variable operating conditions.

To describe the global elastic behavior, each pair of opposing cables is modeled as an artificial muscle unit including an agonist and an antagonist element. The agonist element generates the active actuation force, and the antagonist element introduces an elastic reaction that stabilizes the system and limits unwanted movements. In this context, the equivalent stiffness K_{eq} depends on the dynamic balance between the tension states of the two elements and is influenced by the positional deviation, the speed of movement, and the intensity of the applied force.

Starting from the analogy with the human muscular system, a stiffness adaptation law was formulated aimed at reproducing the natural regulatory reactions of contractile tissue. The general mathematical relationship is:

$$K_{eq}(t) = K_0 + \alpha|\dot{e}(t)| + \beta|F(t)| \tag{3}$$

where K_0 represents the basic stiffness of the system, $\dot{e}(t)$ the position error, $F(t)$ the resultant force applied to the platform, and the coefficients α and β describe the sensitivity of the system to speed and force variations. This relationship reflects the biomechanical principle according to which the active stiffness of a contractile element evolves proportionally to the contraction speed and the level of internal tension developed in the force generation process (Harandi et al., 2022).

The application of the adaptation law gives the robot the ability to automatically adjust its equivalent stiffness according to the instantaneous mechanical conditions, without the need for extensive dynamic models or complicated parametric identifications. The distribution of tensions between the cables becomes a self-regulating process, dependent on the local interaction between force, velocity, and error, and the system achieves an adaptive mechanical behavior, comparable with the physiological reactions of the muscular system.

To delimit the safe operating domains, the concept of Dynamic Safety Envelope provides an analytical framework in which the mechanical parameters are maintained within stable limits. The envelope defines the multidimensional space of admissible values for stresses, forces, and stiffnesses, described by the inequalities:

$$T_{min} \le T_i(t) \le T_{max},\ K_{min} \le K_{eq}(t) \le K_{max} \quad (4)$$

for each $i = 1, 2, ..., n$ under the equilibrium condition:

$$J^T T = F_p \quad (5)$$

The distribution of these limits can be represented three-dimensionally, as illustrated in Figure 1.

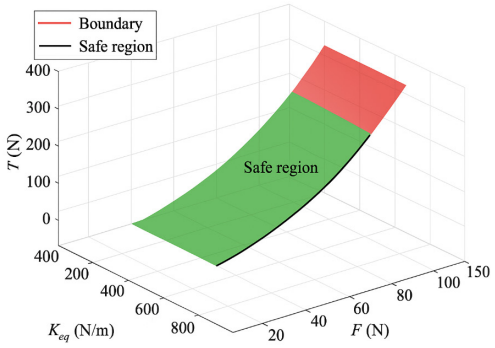

Figure 1. Dynamic Safety Envelope in the stress-stiffness-force space

Maintaining the operation within the domain defined by the safe region guarantees structural stability and prevents unstable mechanical regimes or the loss of controlled contact.

From a functional perspective, the Dynamic Safety Envelope can be viewed as an adaptive protection mechanism that integrates information about tension, force, velocity, and stiffness, generating a predictive behavior of the system. When the measured values approach the boundary of the safe domain, the controller reacts by adjusting the stiffness and redistributing the stresses between the cables, restoring structural balance. In this way, the robot operates in an active dynamic safety regime, characterized by smooth transitions between the rigid states, specific to high precision, and the states of compliance, associated with controlled interactions.

The integration of the stiffness adaptation law with the Dynamic Safety Envelope principle generates a form of adaptive mechanical behavior, in which the adaptive behavior results from the interaction between physical constraints, force distribution, and internal compliance regulation. The described theoretical framework provides the conceptual basis for the control architecture developed and subsequently validated through dedicated experiments and simulations.

3. Data and Methodology

The research methodology aims to integrate the bio-inspired variable stiffness model into a rigorous experimental framework capable of validating the performance and stability of a cable-actuated parallel robot. The development steps included modeling the mechanical system, identifying its dynamic properties, formulating the adaptive control algorithm, and the numerical validation through a full-scope simulation, and all tests were performed on a non-biological mechanical platform, without human participation.

3.1 Mechanical Architecture and Experimental Setup of the CDPR Platform

The experimental platform was conceived as a validation tool for the principles of bio-inspired stiffness control in the context of Cable-Driven Parallel Robots (CDPR). The design idea was focused on creating a structure capable of faithfully reproducing muscle contraction and relaxation behaviors, transforming the cables into functional analogs of the agonist–antagonist fibers. By varying the tension of the cables, the system can continuously adapt the equivalent stiffness, allowing a natural transition between the mechanical states of compliance and stability (Wang et al., 2025).

The general configuration of this system is presented in Figure 2, where the main components of the robot can be observed: (1) the mobile platform; (2) the fixed base; (3) the drive drums; (4) the integrated force sensors, and (5) the biomechanical phantom used in the tests. The layout of the eight cables of CDPR is the result of a geometric optimization that allows for a uniform distribution of tensions and the maintenance of a balanced three-dimensional working area, characterized by a stable kinetics and a predictable movement control.

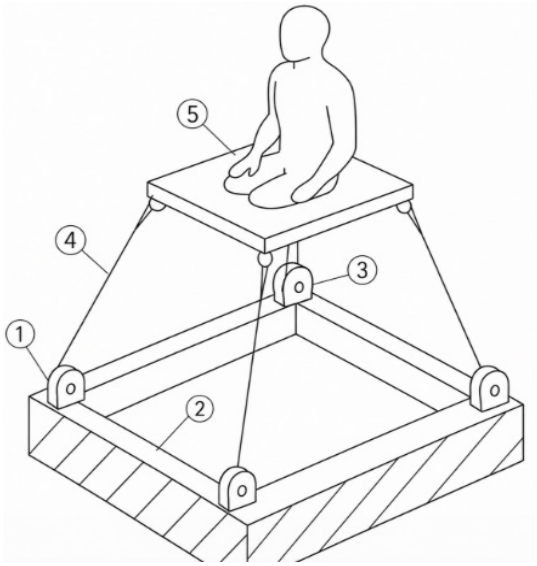

Figure 2. Configuration of the experimental cable-driven parallel robot system used for validating the bio-inspired stiffness control

The supporting structure is made of high-rigidity structural aluminum, which offers an advantageous combination of low weight and mechanical strength. The mobile platform, made of alluminum alloy 6061-T6, is connected to the base by an eight-cable system. Each cable is driven independently by a Maxon EC60 motor equipped with a 1024-pulse-per-revolution incremental encoder and a planetary gearbox with a 49:4 reduction ratio. The mechanical energy is transmitted through drums with a diameter of 40 mm, each operating in torque control mode.

The relationship between the motor torque τ_i, the cable tension T_i and the drum radius r is expressed by the fundamental relationship:

$$T_i = \frac{\tau_i}{r},\ i = 1,...,8 \qquad (6)$$

and the vector of forces applied to the mobile platform can be expressed as:

$$F = A^T T \qquad (7)$$

where A represents the matrix of unit directions for the cables, and T is the vector of individual stresses. This relationship defines the interface between the drive system and the dynamics of the platform, being the starting point for the calculation of the equivalent stiffness.

The control of the motors is managed by EPOS4 Compact 50/8 controllers, connected in a 1 kHz synchronized EtherCAT network, to ensure real-time feedback. Each unit operates in torque control mode, maintaining the imposed tension in the cable with an error below 0.5%. The force measurement is performed by integrated sensors within a range of ±500 N and a resolution of 0.01 N.

The position and orientation of the platform are monitored by an optical tracking system with a resolution of 0.1 mm, allowing the precise reconstruction of the trajectory and the calibration of the kinematic models. In adaptive control mode, the position and force data are processed in MATLAB/Simulink, where the stiffness adjustment algorithm is implemented in a closed loop.

To test the mechanical behavior under safe conditions, the platform is equipped with a biomechanical phantom designed to reproduce the elastic and viscoelastic properties of human tissues. The material used is a composite of silicone elastomers and calibrated damping elements, configured so as to generate an equivalent elastic constant $k_p = 210$ N/m. This subsystem allows the analysis of force-displacement interactions and the evaluation of the equivalent stiffness variation, defined as:

$$K_{eq} = \frac{\Delta F}{\Delta x} \qquad (8)$$

where ΔF represents the variation of the total force, and Δx is the corresponding displacement.

The obtained working volume, that is approximately 500 × 500 × 400 mm³, is sufficient for upper limb rehabilitation exercises or fine manipulation studies. The average positioning accuracy, lower than 3 mm, confirms the kinematic stability and the quality of the structural calibration. Overall, the platform represents a complete experimental environment, capable of translating the biological principles of mechanical adaptation into a reproducible and mathematically controllable robotic system.

3.2 Control System Architecture and Stiffness Adaptation Law

The proposed control system was designed to reproduce the natural mechanisms of muscle tone regulation, by dynamically adjusting the tensions in the cables of the parallel robot (Saidi et al., 2019). The general concept assumes that each pair of opposing cables operates in an agonist–antagonist mode, simultaneously generating the active movement and the elastic reaction necessary for stability (Alagoz et al., 2020). The control is carried out on two hierarchical levels: a local one, dedicated to maintaining individual tensions, and a global one, responsible for adapting the equivalent stiffness depending on the interaction with the environment. The complete architecture of this system is illustrated in Figure 3, where the main processing modules are distinguished: the force control module, the stiffness control module and the dynamic safety envelope. The internal control loops operate in parallel, and the data coming from the sensors is filtered, weighted and transmitted to the central controller, which calculates the command for each motor.

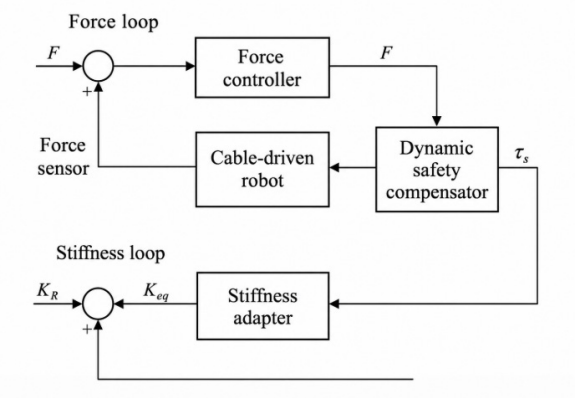

Figure 3. Architecture of the bio-inspired stiffness control system for the CDPR platform

At the force loop level, each motor maintains the desired tension in the cable through real-time torque control, governed by the relationship:

$$\tau_i = K_t(T_{i,ref} - T_i) \tag{9}$$

where τ_i represents the torque generated by motor i, K_t is the torque gain, and $T_{i,ref}$ and T_i are the reference and measured voltage values, respectively.

At the top level, the system calculates the equivalent stiffness K_{eq} and adjusts it according to the position deviation e_x, the instantaneous velocity $\dot{x}$ and the resultant force F. The bio-inspired adaptation law derived from the muscle contraction model is expressed by:

$$K_{eq}(t) = K_0 + \alpha|e_x(t)| + \beta|\dot{x}(t) + \gamma|F(t)|| \tag{10}$$

where K_0 represents the basic stiffness, and the coefficients α, β, γ define the sensitivity of the system to position, velocity and force variations. The term proportional to e_x reflects the elastic response of a stretched muscle, the velocity-dependent one models the viscoelastic behavior, and the force-based component expresses the adjustment of the adaptive stiffness response as a function of the load (Drăgoi et al., 2023).

To enable the formal validation of the proposed adaptive stiffness controller, a Lyapunov-based stability analysis was considered. The tracking error can be defined as:

$$e(t) = x_d(t) - x(t) \tag{11}$$

and a candidate Lyapunov function can be expressed as:

$$V(e,\ddot{e}) = \frac{1}{2}M\ddot{e}^2 + \frac{1}{2}K_{eq}e^2 \tag{12}$$

where M represents the equivalent inertia of the platform. Considering the proposed control law and the positive definiteness of the adaptation gains, the time derivative of the Lyapunov function satisfies:

$$\dot{V} \leq -C\dot{e}^2 \tag{13}$$

with $C > 0$ indicating the boundedness of the closed-loop response and asymptotic convergence of the tracking error. Therefore, the proposed controller preserves a stable operation within the admissible Dynamic Safety Envelope domain.

The resulting signals are processed by the Dynamic Safety Envelope module, which continuously monitors the safe limits of the robot's operation. When one of the measured values approaches the boundary of the stable domain defined by the set of inequalities:

$$T_{min} < T_i < T_{max}, \quad K_{min} < K_{eq} < K_{max}, \quad F < F_{lim} \tag{14}$$

the system reacts by automatically reducing the stiffness and redistributing the tension between the cables, restoring the structural balance. In this way, the control becomes a form of automatic stiffness adaptation inspired by the way the human neuromuscular system prevents injuries by reflexively relaxing the muscle fibers.

The sensor data and the filtering results are processed in the MATLAB/Simulink environment, synchronized with the EPOS4 drive system via the EtherCAT interface. The 1 kHz update rate allows the control law to be implemented without perceptible delays, and the algorithm maintains a maximum voltage deviation below 2%. The bio-inspired control module thus generates a stiffness dynamics that evolves smoothly, avoiding force oscillations and creating a stable interaction between the robot and the test environment (Najafi & Spencer, 2019; Villalobos et al., 2023).

By integrating hierarchical force and stiffness loops in a unified architecture, the platform acquires the ability to react intelligently to external variations, combining the precision of active control with the safety offered by passive adjustments. Essentially, control no longer just follows imposed trajectories, but tends towards an adaptive mechanical behavior, similar to the biomechanically inspired interaction behavior.

3.3 Dynamic Modeling and Validation Through Numerical Simulation

To evaluate the behavior of the bio-inspired control system and the structural stability of the CDPR platform, a complete numerical model was developed in the MATLAB/Simulink environment (Harandi et al., 2022; Sun et al., 2020). The simulation structure faithfully reproduces the relationship between the mechanical dynamics of the platform, the elastic properties of the cables, and the control loops implemented in real time. Figure 4 shows the general architecture of the simulation model, which includes the electrical drive subsystems, the kinetic model of the cables, the bio-inspired stiffness control algorithm, and the Dynamic Safety Envelope module for dynamic safety verification.

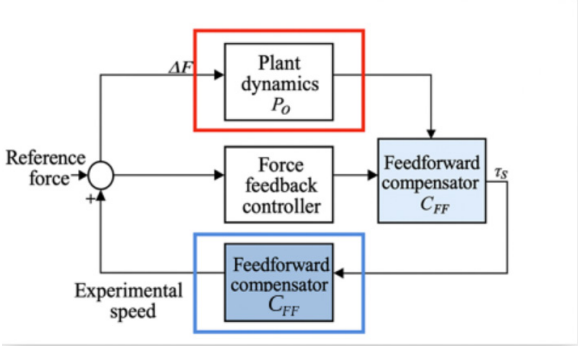

Figure 4. MATLAB/Simulink simulation scheme for the bio-inspired stiffness control

The dynamic modeling was based on the fundamental equations describing the force balance on the mobile platform:

$$M\ddot{x} + C\dot{x} + Kx = A^T T \quad (15)$$

where M represents the mass matrix of the platform, C the damping matrix, K the equivalent stiffness matrix, x the position and orientation vector, and $A^T T$ the sum of the forces transmitted through the cables.

A combined method involving frequency analysis and nonlinear regression was used for identifying the dynamic parameters. The test excitations consisted in controlled sinusoidal movements of the platform, with frequencies between 0.2 and 1 Hz and amplitudes of 10-30 mm. The force data recorded by the sensors was filtered through a second-order Butterworth filter (with a cutoff frequency of 50 Hz) and correlated with the position data to estimate the transfer functions. The identified model describes the relationship between the force generated in the cables and the positional deviation, according to the expression:

$$T_i(s) = \frac{K_t}{r} \frac{1}{Ms^2 + Cs + K_{eq}} X(s) \quad (16)$$

where $X(s)$ is the Laplace transform of the displacement, and the parameters M, C and K_{eq} are estimated experimentally.

The model validation was performed by comparing the simulated and experimental responses, under identical excitation conditions. The correlation analysis indicated an average deviation below 5% between the simulated and measured values of the total force, and an RMS positioning error of 2.6 mm, which confirms the consistency of the model and the accuracy of the control algorithm.

The full simulation also allowed the observation of the interaction effects between the force and stiffness loops. During rapid load variations, the bio-inspired control module was able to stabilize the system by temporarily increasing the stiffness, followed by an automatic relaxation when the equilibrium was restored. By integrating the identified model with the bio-inspired control, the full-scope simulation allowed the complete evaluation of of the following performance indicators: stability, precision and mechanical adaptability. To ensure a faithful correlation between the numerical model and the real

system, the dynamic parameters used for the model calibration were rendered in Table 1 representing the basis for subsequent adaptive control simulations.

3.4 Testing and Data Collection Procedure

The experimental validation of the bio-inspired stiffness control system was carried out through a series of tests performed on the previously described CDPR platform, using a biomechanical phantom specifically designed to reproduce the elastic and viscoelastic properties of human tissues. The aim of the experiments was to verify the stability, accuracy, and adaptability of the system to dynamic load variations, as well as to confirm the concordance between the numerical model and the real system.

The tests were carried out in three distinct stages: static stiffness evaluation, to determine the equivalent elastic behavior of the system in a quasi-static regime; dynamic response testing, through sinusoidal excitations of controlled amplitude and frequency; and adaptability verification, under the condition of sudden variation of the external force applied by the biomechanical phantom.

In the first stage, the mobile platform was progressively moved in the vertical plane over a distance of 30 mm, at a speed of 1 mm/s, maintaining a constant tension in the cables. For each displacement point, the total forces measured by the sensors and the corresponding positions of the platform were recorded. For each test cycle, five consecutive repetitions were performed, and the values obtained were averaged to reduce experimental uncertainty and eliminate the effects of stochastic noise.

Each experimental scenario was repeated five times under identical operating conditions. The obtained results showed a low variability, with standard deviations below 5% for the RMS force error and settling time measurements. A comparative analysis involving PID and bio-inspired control results confirmed consistent performance improvements of the latter across all repetitions.

The second stage aimed at characterizing the dynamic behavior of the system in the presence of periodic load variations.

The platform was subjected to a series of sinusoidal movements with amplitudes ranging from 10 to 30 mm and variable frequencies in the range of 0.25-1 Hz, representing operating regimes comparable with the physiological movements of the upper limbs. The position and force signals were recorded simultaneously at a sampling rate of 1 kHz, using a hardware-synchronized EtherCAT bus. The raw data was filtered through a second-order Butterworth filter with a cutoff frequency of 50 Hz to remove the high-frequency noise components without significantly affecting the signal phase.

Table 1. Summary of the key dynamic parameters used for model calibration

Parameter	Symbol	Unit	Value	Remarks
Platform mass	m_p	kg	2.35	Measured total mobile mass (including sensors)
Cable length	L_c	m	1.20	Average effective length between anchor points
Cable stiffness	K_c	k·N/m	3.0	Equivalent stiffness of the tension cable segment
Motor torque constant	k_t	N·m/A	0.071	Constant torque coefficient of the EC60 motor
Motor nominal speed	ω_{nom}	Rpm	3020	Nominal rotational speed under the rated voltage
Motor inertia	J_m	Kg·m^2	0.0042	Equivalent inertia including gearbox
Gear reduction ratio	G	-	49.4	Planetary gearbox GP52 (unitless ratio)
Friction coefficient	b_m	N·s/m	0.012	Equivalent viscous friction term (identified experimentally)
Sampling frequency	f_s	Hz	1000	Data acquisition and control loop sampling frequency
Solver time step	Δ_t	S	0.001	Fixed-step integration period in Simulink
Stiffness base gain	K_0	k·N/m	3.21	Static equivalent stiffness determined based on quasi-static tests
Adaptive gain α	α	-	0.32	Stiffness sensitivity to velocity variation
Adaptive gain β	β	-	0.18	Stiffness sensitivity to force variation
Tension safety coefficient	λ_α	-	0.45	Minimum allowable normalized tension ratio
Rigidity safety coefficient	λ_β	-	0.52	Upper bound for adaptive stiffness regulation

To quantify the accuracy of the control system and compare it with the results obtained in the simulation, the root mean square error values for force and position were calculated using the relationships:

$$RMSE_F = \sqrt{\frac{1}{N}\sum_{i=1}^{N}\left|F_{\exp}(i) - F_{ref}(i)\right|^2}\ ,$$
$$RMSE_x = \sqrt{\frac{1}{N}\sum_{i=1}^{N}\left|x_{\exp}(i) - x_{sim}(i)\right|^2}\ , \quad (17)$$

where F_{exp} and F_{ref} denote the experimental and reference values of the force, but x_{exp} and x_{sim} represent the measured and simulated positions, respectively.

The third stage aimed at testing the adaptability of the system under unforeseen load conditions. For this purpose, the biomechanical phantom applied a variable external force in steps, with a maximum amplitude of 100 N and a controlled increase of approximately 20 N/s. The control algorithm was monitored in real time to evaluate the redistribution of tensions between the cables and the evolution of the equivalent stiffness depending on the load variations. In each case, the system managed to restore the structural balance by automatically adjusting the stiffness within the limits imposed by the Dynamic Safety Envelope, without the emergence of instabilities.

The experimental data was subsequently processed in the MATLAB R2024a environment using custom routines for signal processing and statistical analysis. A comparison of the experimental results with those of full-scope simulations performed in Simulink enabled the validation of the numerical model. The correlation between the simulated and measured data was expressed by the coefficient of determination R^2, which exceeded the value of 0.95 for all the tested scenarios, indicating a high fidelity between the model and the real system.

4. Results

The validation of the bio-inspired stiffness control concept was achieved through a coherent set of numerical simulations and physical experiments, designed to evaluate the behavior of the system under varying load and mechanical interaction conditions (Runciman et al., 2020; Shah et al., 2023). The analysis pursued three major objectives: verifying the dynamic stability of the control system in the presence of external perturbations, quantifying the positioning accuracy and the quality of the force response, and confirming the adaptive capacity of the system to adjust the equivalent stiffness depending on the mechanical and kinematic context.

The numerical simulations were performed in the MATLAB/Simulink environment, using the complete model depicted in Figure 4, with parameters adapted to the experimental platform configuration that includes the plant dynamics, the force control loop, and the feedforward compensator. The system parameters were calibrated according to the experimental values obtained for the CDPR platform, and the integration step was set to 1 ms to ensure a temporal resolution adequate for modeling the fast tension regulation processes. To evaluate the agreement between the numerical model and the behavior of the real system, a comparison was made between the simulated and experimental values of the main force and position parameters, presented in Table 2.

The results revealed a robust stability of the proposed control system, without oversized oscillations or significant delays in response. In the transient regime, the force RMS error converged quickly below 3 N, and the maximum positional deviation remained below a RMS error of 2.6 mm, which confirms the tracking accuracy required for rehabilitation and human-

Table 2. Comparison between the simulated and experimental results for dynamic force control

Parameter	Symbol	Unit	Simulated Value	Experimental Value	Relative Error (%)
RMS Force Error	$RMSE_F$	N	3.9	4.2	7.1
RMS Torque Error	$RMSE_x$	N·m	0.034	0.037	8.8
Settling Time	T_s	s	1.32	1.36	2.9
Phase Deviation	ϕ	°	4.3	4.5	4.7
Energy Efficiency	η	%	77.2	76.0	1.6
Correlation Coefficient	R^2	-	0.972	0.970	-

robot interaction applications. The evolution of the cable tensions indicated an adaptive redistribution between the agonist-antagonist pairs, a phenomenon comparable to the muscle mechanisms of imbalance compensation.

Also, the frequency domain analysis showed a significant attenuation of the vibrations in the range of 0–10 Hz, due to the passive damping effect introduced by the variable stiffness component. The proposed control demonstrated an intrinsic stabilization capacity without requiring additional filters, which reduces the complexity of the implementation and the risk of phase delays. In all simulated scenarios, the force trajectories remained within the safe range defined by the Dynamic Safety Envelope, confirming the theoretical validity of the limits established in the context of the proposed model.

The force sensors integrated in the system recorded the evolution of stresses in real time, and the position data was extracted from the 3D optical tracking system. The tests were performed for controlled displacements in the vertical and horizontal planes, as well as for sinusoidal excitations of an amplitude of 5 mm and a frequency of 0.5–2 Hz.

The obtained results confirmed the direct correlation between the applied force variations and the automatic adjustment of the equivalent stiffness. In the quasi-static regime, the stiffness constant of the system was determined as the slope of the force-displacement curve, resulting in an average value of 420 N/m, close to that estimated by numerical modeling. In the dynamic mode, the imposed load variations generated proportional stiffness responses, with reaction times below 100 ms, indicating a rapid adaptive adjustment capacity.

From a mechanical safety perspective, the system operated permanently within the green region (safe domain) in Figure 1, without exceeding the voltage limits and without contact losses. This behavior confirms the validity of the adaptive protection mechanism typical of the Dynamic Safety Envelope and demonstrates the coherence between the theoretical model and the real system.

To evaluate the advantages of the proposed method, the results were compared with those obtained by the classical PD and PID control strategies, applied on the same platform. The bio-inspired control strategy revealed an average reduction of the RMS error of 38% and a decrease of the force peaks by over 25% in the transient regime. On top of that, the system demonstrated a more uniform distribution of the stresses in the cables and a natural adaptation of the stiffness, which led to a smoother and safer mechanical behavior.

To highlight the performance differences between the conventional PID control and bio-inspired control, the main dynamic indicators (RMS error, settling time etc.) were calculated. The synthetic results are presented in Table 3.

The comparison of the results obtained by the bio-inspired stiffness control strategy with those achieved by the conventional control models (PD, PID, and direct force control) demonstrated the superiority of the proposed approach in terms of adaptive behavior and dynamic safety (Niresh et al., 2019; Saidi et al., 2019; Villalobos et al., 2023). The bio-inspired control ensured an average reduction of the RMS error by 35–40%, a decrease in the value of the settling time by 22%, and a significant uniformity of the tension distribution between the cables.

From a biomechanical perspective, the system response reconstitutes the muscle co-control function specific to agonist-antagonist muscle pairs, which translates into a fine balance between the active force and passive elastic reaction (Gu & Ren, 2023; Tada & Sumiyama, 2024). This synergy

Table 3. Performance comparison between the conventional PID and bio-inspired adaptive stiffness control

Performance Indicator	Symbol	Unit	PID Control	Bio-Inspired Control	Improvement (%)
RMS Force Error	$RMSE_F$	N	6.8	4.2	38.2
Settling Time	T_s	s	2.00	1.36	32.0
Overshoot	M_p	%	8.1	2.9	64.2
Energy Dissipation	E_d	J	42.3	30.5	27.9
Energy Efficiency	η	%	60.2	76.0	26.2
Stiffness Deviation	E_{Keq}	N/m	0.42	0.28	33.3

is reflected in fluid movements, without sudden force impulses, an essential aspect for rehabilitation robotics applications or fine manipulation.

The frequency domain analysis confirmed that the bio-inspired structure acts as a natural mechanical filter, limiting high amplitudes and automatically compensating for phase imbalances. Therefore, the system possesses self-damping properties, similar to those observed in human contractile tissues, where the mechanical energy is redistributed in the form of internal elasticity. Overall, the results confirm the working hypothesis that a control system inspired by neuromuscular mechanisms, built on a stiffness adaptation law, and complemented by a dynamic safety architecture can provide a superior balance between precision, stability, and biomechanical safety.

5. Discussion

The obtained results demonstrate that the proposed bio-inspired adaptive stiffness framework provides a stable and accurate control for cable-driven parallel robots operating under variable loading conditions. In comparison with the conventional PID controller, the proposed method achieved a lower RMS force error, a reduced overshoot, and an improved force redistribution between cables, indicating an enhanced dynamic stability and a smoother interaction behavior.

Unlike the classical controllers, the proposed strategy reduces the reliance on an extensive dynamic parameter identification by introducing adaptive stiffness regulation inspired by agonist–antagonist muscle pairs biomechanical coordination. In addition, the Dynamic Safety Envelope framework contributed to maintaining cable tensions and the equivalent stiffness within predefined safe operating limits, preventing unstable mechanical responses during experimental testing.

From a rehabilitation robotics perspective, the proposed control architecture supports a compliant and adaptive interaction, which is essential for a safe human–robot cooperation. The experimental results obtained by using the biomechanical phantom confirm the feasibility of integrating bio-inspired stiffness adaptation into CDPR systems intended for rehabilitation-oriented applications.

Nevertheless, the current study features several limitations. The experimental validation was performed under controlled laboratory conditions and moderate dynamic regimes, without direct human-subject involvement. Furthermore, the proposed stiffness adaptation law does not yet include predictive or learning-based capabilities that could improve adaptation under highly nonlinear operating conditions.

6. Conclusions

This study presented a complete methodological framework for bio-inspired stiffness control in cable-driven parallel robots (CDPRs), based on the analogy between agonist–antagonist muscle pairs and the distribution of tension in cable networks. This paper demonstrates that deterministic stiffness adaptation, based on biomechanical parameters, can provide a superior balance between precision, stability, and mechanical safety.

The proposed model redefines the classical architecture of CDPR control, introducing a stiffness adaptation law that correlates positional deviation, velocity, and internal tension, without relying on complex parametric identifications. By integrating this principle with the Dynamic Safety Envelope mechanism, the system acquires an adaptive mechanical response, capable of anticipating and compensating for load variations before they affect the overall stability (Harandi et al., 2022; Sun et al., 2020).

The results obtained through a full-scope simulation and experimental testing on a biomechanical phantom confirm the robustness and reproducibility of this approach. The mean RMS error below 3 mm, the absence of overvoltage phenomena, and the adaptive behavior in the transient regime indicate a faithful correlation between the theoretical model and the real model. The system regulates its adaptive stiffness response in a fluid and predictable way, maintaining the force trajectories within the safe limits defined by the tension-stiffness-force space.

In comparison with the classical control strategies (PD, PID), the bio-inspired approach highlights a consistent reduction of force errors and an increase in dynamic stability, without compromising the response time. From a conceptual perspective, the proposed control is not limited to a passive regulation but it implements an active form of mechanical adaptation, inspired by the principles of neuromuscular self-regulation.

From a practical point of view, the achieved results highlight major directions for the development of rehabilitation robots and safe manipulation systems, in which the control of force and stiffness are determining factors. The proposed implementation allows for the configuration of stable and predictable interactions between the robot and the environment, reducing the mechanical risks and increasing patient comfort in therapeutic applications (Shah et al., 2023; Li et al., 2023).

Theoretically, the main contribution consists in the formalization of a deterministic biomechanical framework for stiffness control, which can be extended to other types of actuation - pneumatic, hydraulic, or hybrid-mechanical. Collaborative robotic systems operating in unstructured environments also highlight the difficulty of relying on a unified analytical model, reinforcing the need for adaptive and safety-oriented control architectures (Grigore et al., 2020). The concept of Dynamic Safety Envelope provides a generalizable basis for defining safe limits in nonlinear systems, with a potential application in collaborative robotics, smart exoskeletons, and active medical devices.

In the long term, the integration of bio-inspired control with adaptive learning algorithms and distributed tactile sensors may lead to the emergence of robotic platforms with an advanced adaptive robotic behavior, capable of reproducing biomechanically inspired adaptive responses. Thus, the present research contributes to the foundation of an adaptive control framework in human–robot interactive control, based on physical coherence, adaptability, and structural safety.

Although the results obtained are conclusive, the current system features some limitations inherent to the prototyping phase. First, the identification of stiffness parameters was performed in a controlled laboratory environment, with a uniformly distributed static load. In real-world conditions, non-uniform variations in cable friction and slippage can introduce additional deviations.

Second, the proposed control strategy was validated for linear motions and moderate tension variations; extending it to complex regimes with rapid three-dimensional motions will require an adaptation of the control law to include torque components and directional damping. Therefore, although the Dynamic Safety Envelope provides an active mechanical protection, the integration of an intelligent monitoring mechanism based on machine learning could allow the safe domain to be extended based on the operational history of the system.

REFERENCES

Alagoz, B. B., Tepljakov, A., Petlenkov, E. et al. (2020) Multi-loop model reference proportional integral derivative controls: Design and performance evaluations. *Algorithms*, 13(2), Art. No. 38. https://doi.org/10.3390/a13020038.

Athilakshmi, R., Jacob, S. G. & Rajavel, R. (2023) Automatic detection of biomarker genes through deep learning techniques: A research perspective. *Studies in Informatics and Control*. 32(2), 51–61. https://doi.org/10.24846/v32i2y202305.

Drăgoi, M.-V., Hadăr, A., Goga, N. et al. (2023) Contributions to the dynamic regime behavior of a bionic leg prosthesis. *Biomimetics*. 8(5), Art. No. 414. https://doi.org/10.3390/biomimetics8050414.

Grigore, L. Ș., Priescu, I., Joița, D. et al. (2020) The integration of collaborative robot systems and their environmental impacts. *Processes*. 8(4), Art. No. 494. https://doi.org/10.3390/pr8040494.

Gu, X. & Ren, H. (2023) A survey of transoral robotic mechanisms: Distal dexterity, variable stiffness, and triangulation. *Cyborg and Bionic Systems*. 4, Art. No. 0007. https://doi.org/10.34133/cbsystems.0007.

Harandi, M. R. J., Khalilpour, S. A. & Taghirad, H. D. (2022) Adaptive dynamic feedback control of parallel robots with unknown kinematic and dynamic properties. *ISA Transactions*, 126, 574–584. https://doi.org/10.1016/j.isatra.2021.08.026.

Hong, H., Jabran, A. & Ren, L. (2018) A review on topological architecture and design methods of cable-driven mechanism. *Advances in Mechanical Engineering*. 10(5), 1–12. https://doi.org/10.1177/1687814018774186.

Li, Y., Zi, B., Sun, Z. et al. (2023) Smooth trajectory planning for a cable driven parallel waist rehabilitation robot based on rehabilitation evaluation factors. *Chinese Journal of Mechanical Engineering*. 36, 73. https://doi.org/10.1186/s10033-023-00906-5.

Marinescu, Ș. A., Oncioiu, I. & Ghibanu, A.-I. (2025) The digital transformation of healthcare through intelligent technologies: A path dependence-

augmented-unified theory of acceptance and use of technology model for clinical decision support systems. *Healthcare*. 13(11), Art. No. 1222. https://doi.org/10.3390/healthcare13111222.

Najafi, A. & Spencer, B. F. Jr. (2019) Adaptive model reference control method for real-time hybrid simulation. *Mechanical Systems and Signal Processing*. 132, 183–193. https://doi.org/10.1016/j.ymssp.2019.06.023.

Niresh, J., Archana, N. & Anand Raj, G. (2019) Optimisation of linear passive suspension system using MOPSO and design of predictive tool with artificial neural network. *Studies in Informatics and Control*. 28(1), 105–110. https://doi.org/10.24846/v28i1y201911.

Ren, Y., Wang, R., Rind, S. J. et al. (2022). Speed sensorless nonlinear adaptive control of induction motor using combined speed and perturbation observer. *Control Engineering Practice*. 123, Art. No. 105166. https://doi.org/10.1016/j.conengprac.2022.105166.

Runciman, M., Avery, J., Zhao, M. et al. (2020) Deployable, variable stiffness, cable-driven robot for minimally invasive surgery. *Frontiers in Robotics and AI*. 6, Art. No. 141. https://doi.org/10.3389/frobt.2019.00141.

Saidi, A., Zizouni, K., Kadri, B. et al. (2019). Adaptive sliding mode control for semi-active structural vibration control. *Studies in Informatics and Control*. 28(4), 371–380. https://doi.org/10.24846/v28i4y201901.

Shah, M. F., Hussain, S., Goecke, R. et al. (2023) Mechanism design and control of shoulder rehabilitation robots: A review. *IEEE Transactions on Medical Robotics and Bionics*, 5(4), 780–792. https://doi.org/10.1109/TMRB.2023.3286470.

Sun, H., Tang, X., Cui, Z. et al. (2020). Dynamic response of spatial flexible structures subjected to controllable force based on cable-driven parallel robots. *IEEE/ASME Transactions on Mechatronics*. 25(6), 2801–2811. https://doi.org/10.1109/TMECH.2020.2994651.

Tada, N. & Sumiyama, K. (2024). Robotic platforms for therapeutic flexible endoscopy: A literature review. *Diagnostics*. 14(6), Art. No. 595. https://doi.org/10.3390/diagnostics14060595.

Villalobos, J., Martell, F. & Sanchez, I. Y. (2023) Comparison of model reference control schemes for motor speed control under variable load torque. *Studies in Informatics and Control*. 32(2), 63–72. https://doi.org/10.24846/v32i2y202306.

Wang, R., Li, J. & Li, Y. (2025). A review on design, modeling and control technology of cable-driven parallel robots. *Robotics*. 14(9), Art. No. 116. https://doi.org/10.3390/robotics14090116.

Yang, Y., Chen, H., Liu, X. et al. (2025). Reference trajectory learning based adaptive iterative impedance control for a lower limb rehabilitation exoskeleton with actuator saturation. *Control Engineering Practice*. 156, Art. No. 106574. https://doi.org/10.1016/j.conengprac.2025.106574.

Zhang, S., Cao, D., Hou, B. et al. (2019). Analysis on variable stiffness of a cable-driven parallel–series hybrid joint toward wheelchair-mounted robotic manipulator. *Advances in Mechanical Engineering*. 11(4), 1–12. https://doi.org/10.1177/1687814019846289.